

NRC Publications Archive Archives des publications du CNRC

Atmospheric plasma sprayed forsterite (Mg_2ASiO_4) coatings: an investigation of the processing-microstructure-performance relationship

Cojocaru, C. V.; Lamarre, J.-M.; Legoux, J.-G.; Marple, B. R.

This publication could be one of several versions: author's original, accepted manuscript or the publisher's version. / La version de cette publication peut être l'une des suivantes : la version prépublication de l'auteur, la version acceptée du manuscrit ou la version de l'éditeur.

For the publisher's version, please access the DOI link below. / Pour consulter la version de l'éditeur, utilisez le lien DOI ci-dessous.

Publisher's version / Version de l'éditeur:

<https://doi.org/10.31399/asm.cp.itsc2012p0384>

ITSC 2012, Thermal Spray 2012: Proceedings from the International Thermal Spray Conference, pp. 384-389, 2012-05-21

NRC Publications Archive Record / Notice des Archives des publications du CNRC :

<https://nrc-publications.canada.ca/eng/view/object/?id=0c7e9f80-69d6-48f6-9d9e-473622323dba>

<https://publications-cnrc.canada.ca/fra/voir/objet/?id=0c7e9f80-69d6-48f6-9d9e-473622323dba>

Access and use of this website and the material on it are subject to the Terms and Conditions set forth at

<https://nrc-publications.canada.ca/eng/copyright>

READ THESE TERMS AND CONDITIONS CAREFULLY BEFORE USING THIS WEBSITE.

L'accès à ce site Web et l'utilisation de son contenu sont assujettis aux conditions présentées dans le site

<https://publications-cnrc.canada.ca/fra/droits>

LISEZ CES CONDITIONS ATTENTIVEMENT AVANT D'UTILISER CE SITE WEB.

Questions? Contact the NRC Publications Archive team at

PublicationsArchive-ArchivesPublications@nrc-cnrc.gc.ca. If you wish to email the authors directly, please see the first page of the publication for their contact information.

Vous avez des questions? Nous pouvons vous aider. Pour communiquer directement avec un auteur, consultez la première page de la revue dans laquelle son article a été publié afin de trouver ses coordonnées. Si vous n'arrivez pas à les repérer, communiquez avec nous à PublicationsArchive-ArchivesPublications@nrc-cnrc.gc.ca.

Atmospheric Plasma Sprayed Forsterite (Mg_2SiO_4) Coatings: an Investigation of the Processing-Microstructure-Performance Relationship

C.V. Cojocar, * J.-M. Lamarre, J.-G. Legoux and B.R. Marple

NRC-IMI, Boucherville, Quebec, Canada

*E-mail: cristian.cojocar@cnrc-nrc.gc.ca

Abstract

Evaluating and understanding the relationship between processing, microstructure and performance of a dielectric coating is essential for its practical usage and reliable application. In this study, the role of the powder feedstock on the properties of atmospheric plasma sprayed forsterite (Mg_2SiO_4) dielectric coatings was investigated by using different forsterite powder cuts. The coatings' microstructural and porosity characteristics associated with the spray conditions employed were assessed via scanning electron microscopy (SEM) and image analysis. The phase composition of the coatings was studied via X-ray diffraction and their crystallinity index determined. The electrical insulating characteristics were investigated using the dielectric breakdown test. The obtained electrical properties were correlated with the microstructural characteristics. Ultimately, a performance comparison between forsterite and other dielectric coatings tested in similar conditions is presented.

Introduction

Atmospheric plasma spraying (APS) represents a versatile and efficient technique to deposit coatings of various materials on large or complex-shaped surfaces and it is widely employed by various industries ranging from automotive, aerospace, oil and gas to electronics. At the same time, plasma spraying allows the deposition of layers ranging from several tens of microns up to millimeters thick, thereby offering a rapid process for producing coatings having a wide range of thicknesses for use in studies of the properties and performance.

Forsterite (Mg_2SiO_4), a synthetic magnesia-silicate ceramic compound (melting temperature $\sim 1900^\circ\text{C}$), is used broadly in electronic ceramic formulations and ceramic-metal seals because of its high coefficient of thermal expansion (CTE) ($11 \times 10^{-6} / ^\circ\text{C}$), comparable to that of some metals, e.g., steel ($13.5 \times 10^{-6} / ^\circ\text{C}$) (Ref. 1). Forsterite has also been found to have very good microwave dielectric properties at high frequencies and thus represents an excellent dielectric material

for millimeter wavelength application in telecommunications and radar systems (Ref. 2-4).

Owing to these attributes, but mostly because of its relatively high value of CTE and thus a smaller mismatch with the CTEs of metallic substrates, forsterite represents a potential candidate as a dielectric coating for various applications. In some instances it could be an alternative to the more conventional alumina, mullite, cordierite or steatite ceramic compounds that are part of the refractory $\text{MgO-Al}_2\text{O}_3\text{-SiO}_2$ family and have a lower CTE (Ref. 5-7), i.e., a larger mismatch with the CTEs of typical metallic substrates. However, research on plasma sprayed forsterite coatings has been rarely reported in the literature (Ref. 5,6,8).

Two decades ago, it was reported for instance that the thermal cycling lifetime of a forsterite top coat plasma sprayed on top of an 80Ni-20Cr bond coated substrate was higher than that of a spinel ($\text{MgO-Al}_2\text{O}_3$) or cordierite coatings (Ref. 5,6). This effect was attributed to a decreased level of thermal stress developed during thermal cycling between the ceramic forsterite and the metallic substrate. However, for many years following those reports no other work on the development of plasma-sprayed coatings emerged in the open literature. It was only very recently that the plasma spraying of forsterite has been revisited (Ref. 8). In that experimental work it was determined that the in-flight particle history and residence time of powder particles of different sizes in the plasma plume had a major effect on the microstructure of the deposited coatings. Nevertheless, the relationship between the processing technique and powder characteristics and the influence of these aspects on the coating microstructure and dielectric properties has not been addressed in depth.

In this work, using different forsterite powder cuts, the role of the powder feedstock on the properties of APS forsterite coatings and the influence on the microstructure and dielectric properties, specifically the dielectric strength, are investigated. A comparison is made with other dielectric plasma sprayed coatings reported in the open literature and with values for forsterite bulk parts.

Experimental

Powder

The starting powder employed in these studies (Du-Co Ceramics, Saxonburg, Pennsylvania, USA) was an agglomerated raw forsterite, un-calcined material (containing an organic binder) produced mainly for use in conventional ceramic pressing and sintering processes to generate bulk forsterite insulator parts.

The microstructure and the size distribution of the powder are presented in Fig. 1a and 1b, respectively. The particle size distribution was evaluated using a laser scattering particle size analyzer (LS 13320, Beckman Coulter, Miami, FL, USA) and found to be in the range 100 – 220 μm .

feedstock for producing dense coatings by the plasma spray process. Large particles do not melt completely and usually the coatings are composed of semi- and un-melted deposits together with voids and other structural defects, leading to highly porous coatings. For this reason the as-received powder was sieved and a size distribution between approximately 44–160 μm used for the preliminary spray trials (see Fig.1b).

In a subsequent set of experiments a finer forsterite powder (obtained after extensive milling procedures of the first powder batch at Du-Co Ceramics) was used to deposit coatings. The microstructure and particle size distribution for this second batch of powder are shown in Fig. 2a and 2b, respectively.

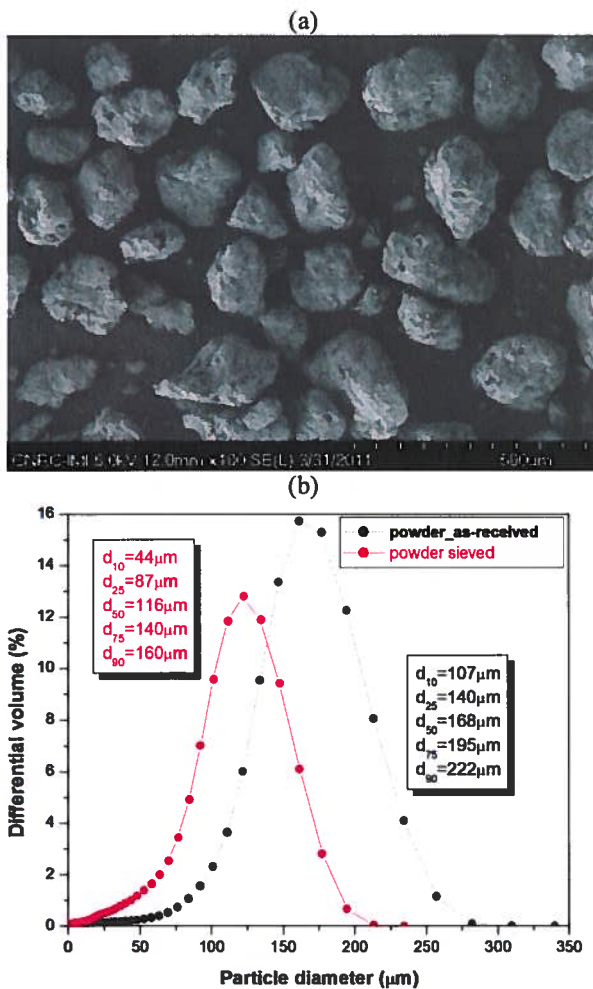


Figure 1: (a) BSE electron micrograph of the as-received forsterite powder and (b) particle size distribution of both the as-received powder and a sieved powder cut used for initial coating production.

Such a coarse size of the powder particles and broad size distribution do not represent a suitable starting material

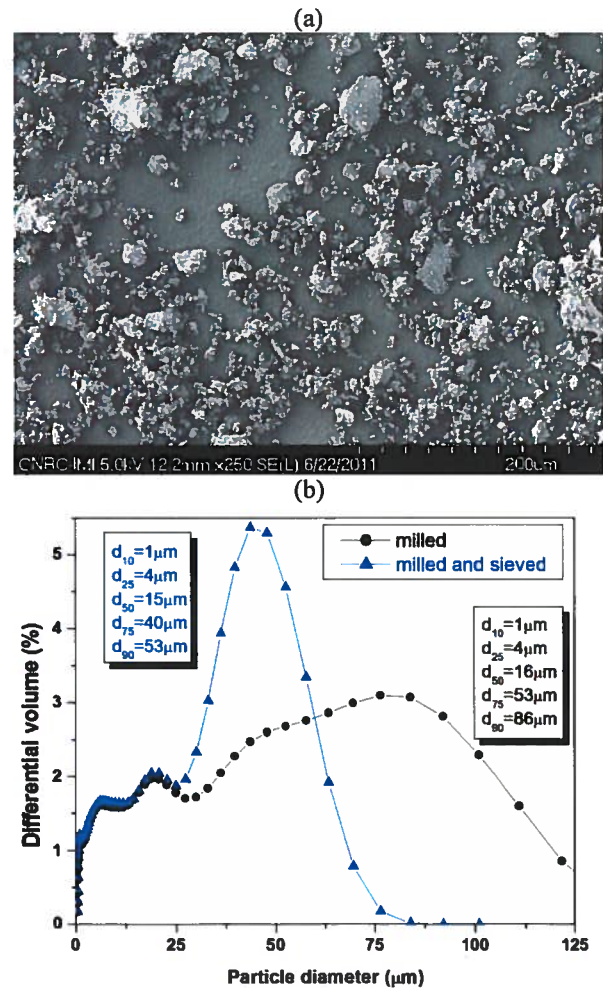


Figure 2: (a) BSE electron micrograph of the milled forsterite powder and (b) particle size distribution of both milled and sieved powder cuts used for coating production.

A third round of tests was conducted using a different powder cut, i.e. -53 microns, obtained from sieving the second batch of the fine-milled powder to produce the size distribution shown in Fig. 2b.

In Table 1 the powder cuts employed to deposit the forsterite coatings are summarized and the coatings labeled accordingly, for further convenience. In the column depicting particle size distribution, data represent maximum and minimum particle size and the diameter corresponding to 50% of the differential volume – particle size distribution function (i.e. d_{50}).

Table 1: Powder cuts used to deposit forsterite coatings and identification of the coatings analyzed.

| Powder cut | Size distribution; d_{50} (microns) | Coating |
|------------|---------------------------------------|--------------|
| A | -160 + 44; 116 | Forsterite A |
| B | -86 + 1; 16 | Forsterite B |
| C | -53 + 1; 15 | Forsterite C |

Sample Preparation

The powders were sprayed on grit-blasted 3 inch x 3 inch mild steel substrates using an APS torch (F4 MB, Sulzer Metco, Westbury, NY, USA). These substrate dimensions were chosen in order to avoid boundary effects during dielectric strength measurements.

In-flight particle temperature and velocity values were measured using an optical sensor (DPV 2000, Tecnar Automation, St. Bruno, QC, Canada) and the coating temperature monitored with a pyrometer. Using slight variations of the torch power and cooling procedure of the substrate, several spray conditions were tested for each powder cut. In Table 1 the general conditions employed to deposit forsterite coatings are summarized. Selected coatings were then chosen for structural and dielectric strength measurements (one sample per spray condition).

Table 2: Atmospheric plasma spray process parameters used to deposit forsterite coatings.

| Parameter | Value |
|-------------------------------------|--|
| Plasma-forming gases and flow rates | Ar, 40 slpm; H ₂ 10 slpm |
| Carrier gas and flow rate | Ar, 3 – 4 slpm |
| Torch power | 32 – 33 kW |
| Cooling | Air, 0 – 50 psi |
| Spray distance | 6.5 – 12 cm |
| Coating thickness | 70 – 300 μ m |

Structural Characterization

The coatings' characteristics (i.e., adherence, cracks and porosity) were evaluated mostly via back-scattered electron (BSE) based microstructural observations. The as-sprayed samples were vacuum impregnated in epoxy prior to cross-section cutting and further prepared by standard metallographic procedures for field-emission scanning electron microscopy (FE-SEM), (Hitachi S4700, Hitachi Ltd., Tokyo, Japan). This FE-SEM, also equipped with an energy

dispersive X-ray (EDX) module, was used to investigate the local elemental composition of the powder and coatings.

Porosity was determined using image analysis of SEM micrographs. One coating was analyzed per spray condition. Ten cross-section SEM images per coating (at magnification 500X) were captured and further binarized. Porosity was measured as area percentage of dark features (pores) using an image analysis software (Visilog 3.5, Leica, Wetzlar, Germany).

The phase composition of the as-sprayed coatings was verified via X-ray diffraction, (XRD), (D8-Discovery, Bruker AXS Inc. Madison, WI, USA) using Cu-K α radiation in Bragg-Brentano (θ - 2θ) configuration. The diffracted signal was collected over a 2θ range of 10° - 90° with a step size of 0.02° and a 5 s/step acquisition time through a 1° fine collimator slit. The index of crystallinity (I_c) of each type of coating was determined using an X-ray diffraction pattern analysis software (EVA, Bruker AXS Inc. Madison, WI, USA).

Dielectric Strength Measurements

Dielectric strength measurements were carried out according to the ASTM D149 standard (Ref. 9) using an in-house developed electrical breakdown setup. One-inch diameter polished stainless steel electrodes with rounded edges were used. Samples were maintained at a temperature of 110°C for 30 minutes prior to and during the test. DC voltage was applied using 30-second steps with increments of 500 V. The precision of the increments was limited by the power supply. Breakdown voltage is reached when the recorded current exceeds 50 μ A. Typically, the measured current goes from below 2 μ A before breakdown to well over 100 μ A right after breakdown. The breakdown voltage can thus be identified easily without ambiguity. Dielectric strength is simply defined by the breakdown voltage divided by the coating thickness.

Results

Coating Microstructure

In the BSE micrograph shown in Figure 3(a) a cross-section of a forsterite coating sprayed with the coarse powder A is depicted. As can be seen the deposited coating appears to have adhered very well to the substrate, however, it is highly porous. The coating presents a high amount of partially and un-melted particles that are indicated by arrows. These features strikingly resemble the microstructures of cross-sections of the powder particles presented in the micrograph in Fig. 3(b) recorded before spraying. The coarse powder shows an agglomerated structure of several constituents and has a rather porous appearance. Elemental analysis of the powder via EDX identified Mg, Si, Sr, O, and C likely due to the presence of MgO, SiO₂, SrO and wax-like organic binders. Some of these particles were deposited during spraying and incorporated into the coating. In some applications such a structure could be an attractive feature. However, for this work it was an undesirable result. Due to the high level of

porosity observed in the forsterite type-A coatings, dielectric strength measurements were not performed.

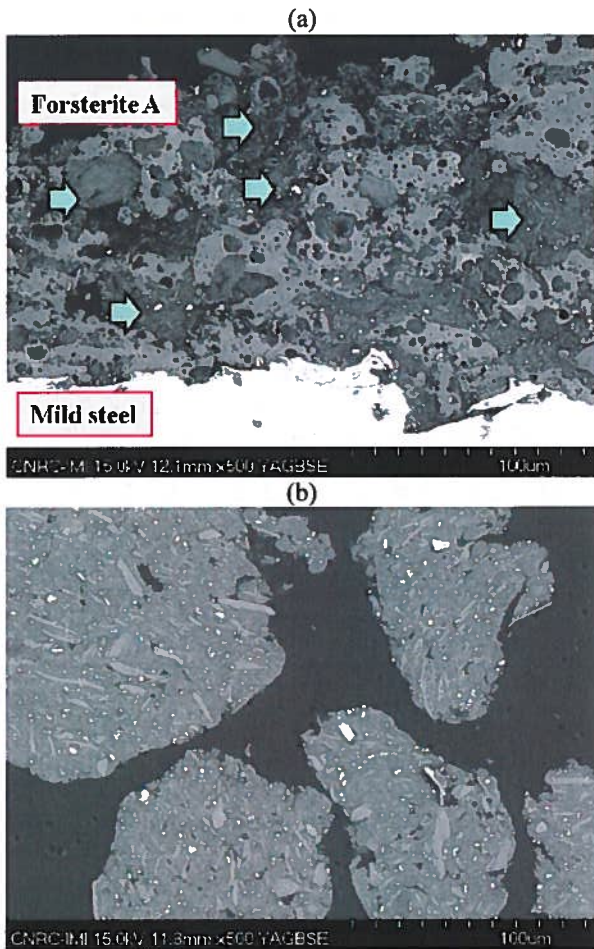


Figure 3: (a) BSE electron micrograph of the forsterite coating produced with a $-150\ \mu\text{m}$ powder cut. (b) Cross-section BSE micrograph of the forsterite particles present in the powder cut A.

In the following, the discussion of the results focuses on the type-B and C forsterite coatings produced after milling and sieving out the large particles. In Fig. 4(a) a cross-section BSE image of a forsterite B-type coating sprayed with the milled powder B is shown. In this case the coating appears to show a higher degree of particle melting and a smaller frequency in the occurrence of un-melted particles (indicated by arrows). Also, the amount of voids found in the forsterite type-A coating was diminished. The porosity present in these coatings, as determined via image analysis, was about 15%. The deposited coating also adhered very well to the substrate and no vertical or horizontal cracking was detected across the cross-section investigated. Coating temperature was kept below 150°C during the spray process using external air cooling (50psi).

In Fig. 4(b) a coating produced after a substrate preheating via 5 passes of the torch (T substrate about 350°C) and using a variation of the cooling procedure (40 psi instead of 50 psi) is shown. Although the density of the coating does not appear to improve significantly, the dielectric strength measurement revealed values close to double of the ones prepared with a higher pressure of air cooling (i.e., 130 kV/cm compared to an average of 60 kV/cm). A heated substrate provides a better platform for the coating crystallization and reduces the amount of the amorphous phase entrapped in the coating due to the slightly prolonged quenching time of the individual droplets. Nevertheless, in some instances (or applications) keeping the substrate temperature at low values is necessary and a preheating procedure might not be suitable.

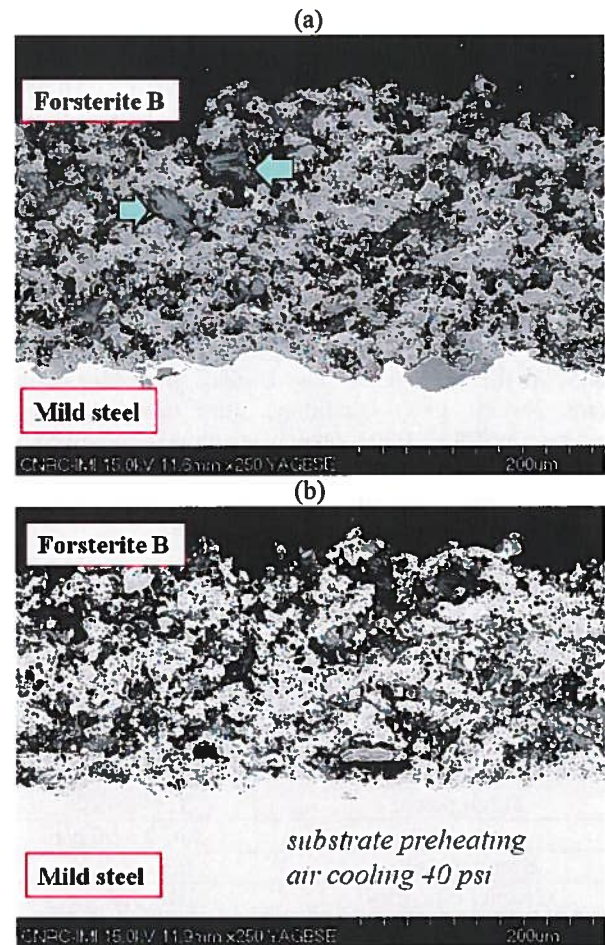


Figure 4: (a) and (b) BSE electron micrographs of the cross-section of forsterite coatings produced using the powder cut B, for two spray conditions.

In Fig. 5 a cross-section BSE image of a forsterite C-type coating sprayed with the milled and sieved powder C is shown. This finest powder cut allowed for the deposition of a coating that exhibited the densest microstructure, associated with the highest degree of particle melting. Nevertheless,

some un-melted particles were still found (indicated in the figure by arrows).

When using the fine C-type forsterite powder a longer spraying time was necessary to deposit coatings with similar thicknesses to those produced when the coarser powder was used. Extended time periods of deposition cause a temperature increase of the coating during spraying. Usually, thermal stresses arising during the cooling phase and caused by coating-substrate mismatch of CTEs generate cracks in the as-sprayed coatings. However, the coatings produced with powder C appear to be free of vertical cracks, thus indicating a fairly good match of the thermal expansion coefficient with the substrate. The deposited coating adhered very well to the substrate. At the same time, within this range of thickness values the porosity of the coatings remained at a relatively high level (i.e., about 13%). Of course this will further influence the insulating performance of the coating.

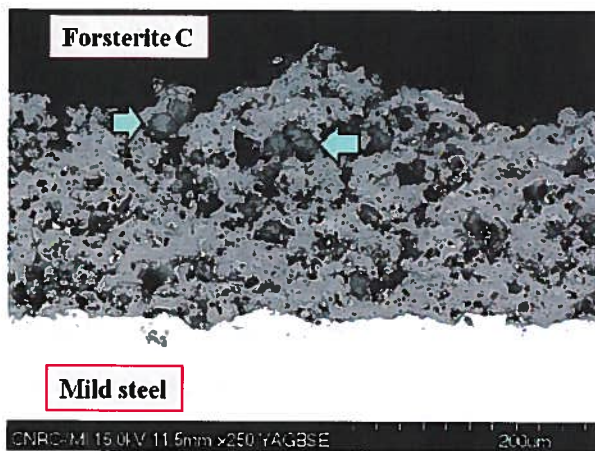


Figure 5: BSE electron micrographs of the cross-section of a forsterite coating produced using the powder cut C.

Dielectric Strength Measurements

For coatings produced with powder B the electrical measurements revealed breakdown voltages between 1.25 kV and 2.25 kV, resulting in dielectric strength values of ~ 60 kV/cm associated with coating thicknesses between 0.02 cm and 0.035 cm. The highest dielectric strength value of 130 kV/cm was obtained for the coatings associated with the spray condition involving the substrate preheating. These values are somewhat lower than values previously reported for alumina plasma sprayed coatings, i.e., 100-175 kV/cm (Ref. 10). The reported value for bulk forsterite sintered ceramic parts produced with this powder formulation is 250 V/mil (i.e., 94.5 kV/cm) (Ref. 11). In the case of the coatings produced with powder C (finest powder), when thinner coatings were produced (average thickness around 0.01 cm), the dielectric strength values averaged 110 kV/cm and reached a high value of about 145 kV/cm (see Fig. 6). In this latter case the porosity of the coating was determined as about 11%. Besides a few

incompletely melted particles still present in the coating microstructure, a particular characteristic of the forsterite-C coatings is the existence of a more accentuated globular porosity (see inset from Fig.6). These may arise due to the presence of MgO in the feedstock. It is known for instance that the thermal spraying of MgO is difficult due to the narrow spread between its values of melting and vaporization temperature (Ref.12). Partial loss by evaporation of the MgO contained in the non-homogeneous powder agglomerates may lead to the formation of these voids during the spray process.

In general, an increase in the coating thickness (for the same spray parameters) resulted in a decrease of the dielectric strength values, mostly due to an increase in porosity and defects within the coating thickness.

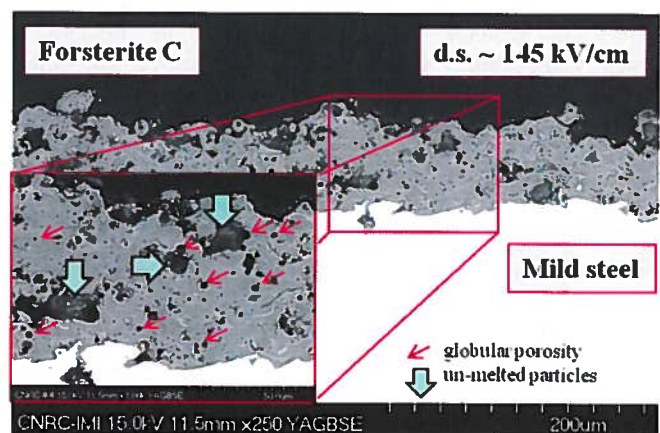


Figure 6: BSE electron micrograph showing details of a thin forsterite coating produced with powder C. (d.s. = dielectric strength)

Structural Analysis

X-ray diffraction patterns of the coatings presented in Fig. 7 reveal a mixture of forsterite, enstatite ($MgSiO_3$) and magnesium oxide crystalline phases and also the presence of an amorphous $nMgO:mSiO_2$ glassy phase. According to the MgO-SiO₂ phase diagram, the forsterite congruent phase is obtained at about 58 wt % MgO (Ref.13). If the initial powder particles are richer in MgO, droplets will re-solidify on the side of the eutectic periclase (MgO) - forsterite (Mg_2SiO_4) ($T \sim 1850^\circ C$). If they are richer in SiO₂ a mixture of enstatite and SiO₂ is favored. The presence of these residual phases is thus attributed to an incongruent melting of the non-homogeneous and broad-sized powder particles during the spraying process. Also it can be observed that coatings produced with the type-A powder contain the highest amount of amorphous phase while coatings produced with the type C powder exhibit the highest degree of crystallinity. To obtain a more quantitative representation of their crystallinity nature, their crystallinity index has been determined using the X-ray diffractograms. The index of crystallinity (I_c), defined as the

ratio between the areas under the Bragg peaks and total areas of the spectrum, was assessed for the region between 2theta angles of 15° and 65° for each type of coating. An increase of the I_c from 0.49 in the case of the forsterite type-A to 0.56 for forsterite type-B and up to 0.79 for forsterite type-C was observed. In this respect, the crystalline structure correlates well with the dielectric insulating performance. The fine-size distribution of the powder feedstock allows for a better melting of the particles residing in the plasma plume and particles will arrive with similar velocities and temperatures on the substrate. In these conditions a more uniform and dense coating is obtained, which in turn provides the desired insulating performance. Consequently, besides the intrinsic spraying process parameters, one of the main contributing factors to achieving good performing forsterite plasma sprayed coatings is the morphology of the powder and its narrow size distribution. Ongoing work is focused on using optimized feedstock to produce high density, crystalline forsterite coatings with further improved dielectric properties and enhanced performance characteristics.

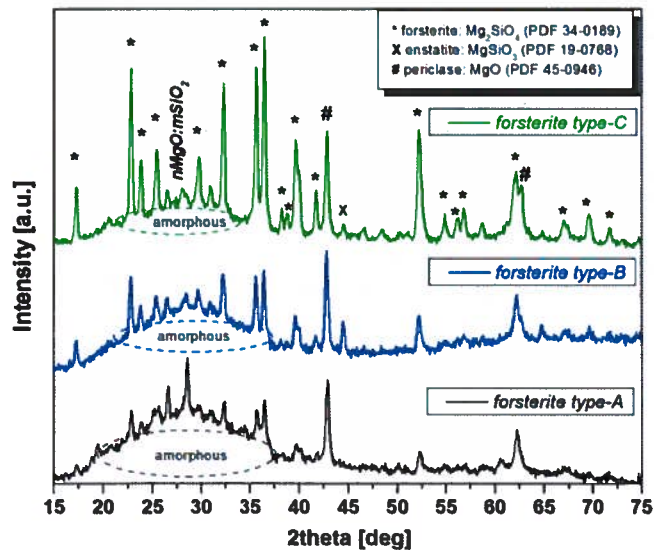


Figure 7: X-ray diffraction patterns of forsterite coatings deposited with powder A, B and C.

Conclusions

Forsterite coatings were plasma sprayed using different size distributions of the powder feedstocks. A good correlation between the feedstock particle size, microstructural appearance of the coating, its crystallinity and dielectric strength performance was observed. As anticipated, less porous coatings exhibited higher values of dielectric strength. It was observed that thinner coatings produced with similar spray conditions showed an increase of the dielectric strength values, due mostly to a decrease in porosity and defects within the coating thickness. Values of dielectric strength up to 145 kV/cm were obtained for the as-sprayed coatings, indicating

that plasma spray is a promising path for obtaining forsterite coatings with the required insulating properties and, at the same time, being more compatible with the substrate.

Acknowledgements

The authors acknowledge valuable technical support from the Surface Technology Group members: J.-C. Tremblay for APS sample production, J. Sykes and D. DeLagrange for metallographic preparation, and M. Thibodeau for SEM imaging.

References

1. W.D. Kingery, H.K. Bowen, D.R. Uhlmann, Introduction to Ceramics (ed.), John & Wiley Sons, New York 1976
2. T. Tsunooka, M. Androu, Y. Higashida, H. Sugiura, and H. Ohsato, Effects of TiO₂ on Sinterability and Dielectric Properties of High Q Forsterite Ceramics, *J. Eur. Ceram. Soc.*, 2003, **23**, p 2573–2578
3. T. Sugiyama, T. Tsunooka, K. Kakimoto, and H. Ohsato, Microwave Dielectric Properties of Forsterite-based Solid Solutions, *J. Eur. Ceram. Soc.*, 2006, **26** p 2097-2100
4. K.X. Song, X.M. Chen, and X.C. Fan, Effects of Mg/Si Ratio on Microwave Dielectric Characteristics of Forsterite Ceramics, *J. Am. Ceram. Soc.*, **90**, (2007) p 1808–1811
5. H.G. Wang, Y.M. Zhu, and H. Herman, Structure of Plasma-sprayed Oxides in the MgO-Al₂O₃-SiO₂ System, *J. of Mat. Sci.*, 1989, **24**, p 4414-4418
6. H.G. Wang and H. Herman, Thermomechanical Properties of Plasma-sprayed Oxides in the MgO-Al₂O₃-SiO₂ System, *Surf. and Coat. Technol.*, 1990, **42** p 203-216
7. P. Ctibor, J. Sedlacek, K. Neufuss, J. Dubsy, and P. Chraska, Dielectric Properties of Plasma-sprayed Silicates, *Ceramic. Int.* 2005, **31**, 315-321
8. H. Samadi, L. Pershin, and T.W. Coyle, Effect of In-flight Particle Properties on Deposition of Air Plasma Sprayed Forsterite, *Surf. and Coat. Technol.*, 2010, **204**, p 3300-3306
9. ASTM D149 - 09 Standard Test Method for Dielectric Breakdown Voltage and Dielectric Strength of Solid Electrical Insulating Materials at Commercial Power Frequencies
10. L. Pawlowski, The Relationship Between Structure and Dielectric Properties in Plasma-sprayed Alumina Coatings, *Surf. and Coat. Technol.*, 1988, **35**, p 285-298
11. <http://www.du-co.com/properties>
12. O. Fukusuma, R. Tagashira, K. Tachino, and H. Mukunoki, Spraying of MgO Films with a Well-controlled Plasma Jet, *Surf. and Coat. Technol.*, 2003, **169-170**, p 579-582
13. F.J.M. Rietmeijer, J.A. Nuth, J.M. Karner, and S.L. Hallenback, Gas-to-Solid Condensation in a Mg-SiO-H₂-O₂ Vapor: Metastable Eutectics in the MgO-SiO₂ Phase Diagram, *Phys. Chem. Chem. Phys.* 2002, **4**, p 546-551